Competition between two types of anti-Stokes emission in Ho^{3+}-activated ZBLAN glass

2009 J. Phys.: Condens. Matter 21 035113

(http://iopscience.iop.org/0953-8984/21/3/035113)

J. Phys.: Condens. Matter **21** (2009) 035113 (4pp) doi:10.1088/0953-8984/21/3/035113

Competition between two types of anti-Stokes emission in Ho^{3+}-activated ZBLAN glass

Cz Koepke[1], K Wisniewski[1,2], D Piatkowski[1] and M Malinowski[3]

[1] Institute of Physics, Nicolaus Copernicus University, Grudziądzka 5, 87-100 Toruń, Poland
[2] Institute of Experimental Physics, University of Gdańsk, Wita Stwosza 57, 80-952 Gdańsk, Poland
[3] Institute of Microelectronics and Optoelectronics, Koszykowa 75, 00-662 Warsaw, Poland

E-mail: koepke@fizyka.umk.pl

Received 5 March 2008, in final form 12 June 2008
Published 11 December 2008
Online at stacks.iop.org/JPhysCM/21/035113

Abstract
A competition between two anti-Stokes emissions has been observed and interpreted in ZBLAN glass activated by Ho^{3+} ions. The first anti-Stokes emission intensity was seen to increase with temperature, whereas another, upconverted emission, was seen to decrease under the same conditions. Both observed tendencies are believed to be caused by the same effect: the multiphonon anti-Stokes excitation of the state responsible for the first emission. Analysis of the kinetics and fits of the theoretical model to experimental data are presented.

(Some figures in this article are in colour only in the electronic version)

1. Introduction

ZBLAN glasses are widely known as very interesting materials for optical fiber communication, especially when activated by rare-earth ions, which can make them good candidates for optical fiber amplifiers or fiber lasers. One of a very promising activators in this respect is the trivalent holmium ion whose features are described in numerous papers (e.g. [1–5]). The Ho^{3+} ion, having a rich variety of energy levels, can be quite an efficient upconverter, yielding the anti-Stokes emissions [6–8]. Investigations of anti-Stokes emissions and their behavior under various conditions (e.g. at various temperatures) are of key importance in the development of new materials for diode-pumped lasers and amplifiers. There are several works concerning the states and transitions involved in such emissions [9–11] (especially upconverted emission from higher states) for Ho^{3+} ions in ZBLAN glasses. A key feature which can cause the upconverted emission is the excited state absorption (ESA) which plays a crucial role when upconverted emission occurs in the frame of one ion [12, 13] (i.e. when no energy transfer happens). In the present work we describe such a situation, which, along with the anti-Stokes excitation [14] can lead to competition between two anti-Stokes emissions.

2. Experimental details

The investigated ZBLAN:Ho^{3+} sample has been prepared by Fiber Labs Co., Japan. The chemical composition of the ZBLAN glass is 53 mol% of ZrF_4, 20% BaF_2, 4% LaF_3, 3% AlF_3, and 20% NaF. The concentration of Ho^{3+} ions in the sample is 2.5 mol%.

Absorption and emission spectra at room temperature (RT) were measured respectively by a Lambda 2 (Perkin-Elmer) spectrometer and the phase sensitive method used also for the ESA spectra measurements. The ESA spectra were measured using a double lock-in technique described in [15] where detailed ESA data are reported. The temperature dependent upconverted emissions were measured using an argon ion laser (ILA-120, Zeiss-Jena) as excitation source and an ORIEL MS125 1/8 m Spectrograph coupled to an InstaSpec II photodiode array detector. We could not perform any decay measurements of the observed anti-Stokes emissions because of the too small intensities of the detected peaks. The sample was heated in an air stream (provided by a heat gun) with the temperature controlled by a thermocouple. In our investigations we could not heat the sample above ~480 K because of the traces of melting and crystallization observed at those temperatures.

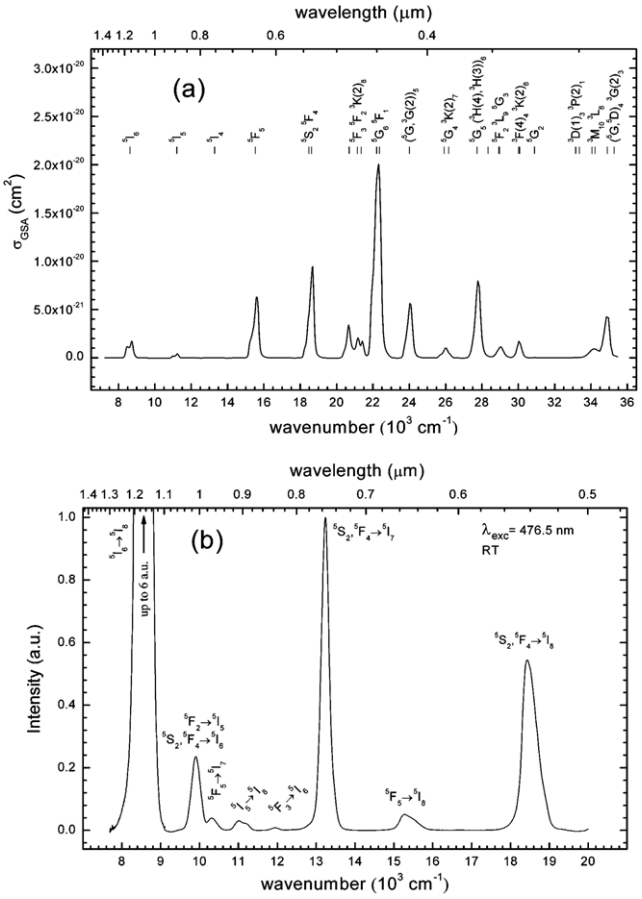

Figure 1. Absorption spectrum (a) and emission spectrum under 476.5 nm excitation (b).

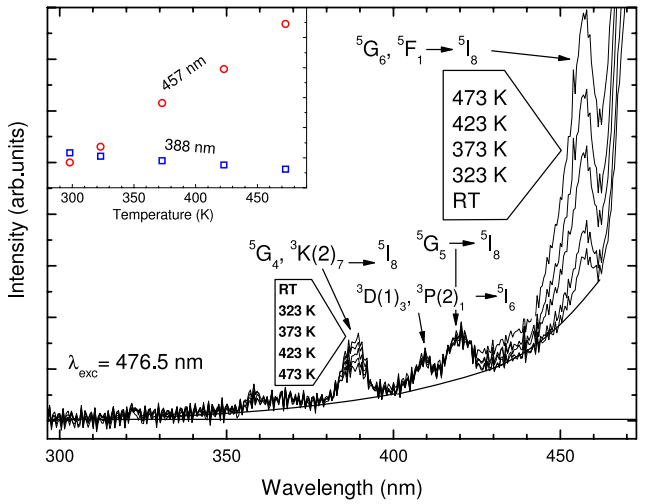

Figure 2. Anti-Stokes emissions and their dependence on temperature. Temperatures are written in the same sequence as corresponding spectra. Inset shows how the intensities of 457 nm and 388 nm emissions alter with temperature.

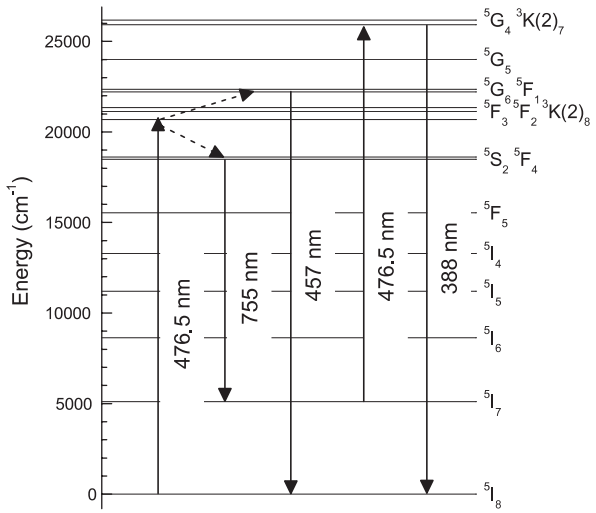

Figure 3. Energy levels/transitions scheme explaining the proposed mechanism of the competition between two anti-Stokes emissions.

3. Results and discussion

Figure 1 presents the absorption and emission spectra (on the Stokes side of excitation) detected at RT in a broad spectral range. Figure 2 illustrates our main result: thermal dependence of the emissions on the anti-Stokes side of the excitation. One can see a distinct increase of the emission, peaking at ∼457 nm, and a simultaneous decrease of the emission, peaking at ∼388 nm. Because all the lines are situated on the slope of the exciting laser line, this 'background' is also depicted in figure 2. The inset in this figure shows the temperature dependence of both emission intensities at the wavelengths of the peaks, after subtraction of the background. Note that in the same temperature range the 457 nm emission grows several times whereas the 388 nm emission does not drop as fast.

In one of our previous papers [16] we described a very similar situation to that mentioned above, namely the 750 nm emission for Nd^{3+} ions in the fluoroaluminate glass. Either the 457 nm emission (Ho^{3+}) or the 750 nm emission (Nd^{3+}) is situated close to the excitation line, which is 476.5 nm in the case of Ho^{3+} and 800 nm in the case of Nd^{3+}; and both are seen to increase with temperature. This observation has suggested to us that in the case of Ho^{3+} we deal with the same mechanism as described in [16] for Nd^{3+} ions. Such a mechanism has been described by Auzel in his classical paper [14], and is called the multiphonon anti-Stokes excitation (MASE). It is perhaps worth noting that the MASE effect, involving 'borrowing' phonons from the host lattice, has already been utilized in the construction of quantum mini-refrigerators [17–19].

Going to the mechanism responsible for the observed thermal characteristics (figure 2), we propose the energy levels/transitions scheme presented in figure 3. The excitation at 476.5 nm (20 986 cm^{-1}) falls into a local minimum of distribution of weakly populating $^5F_3$, $^5F_2$, $^3K(2)_8$ states. From this point the population can be transferred to other states in two ways: in a natural way by radiationless transition (multiphonon relaxation) to lower lying states $^5S_2$, $^5F_4$, and then followed by radiative transition $^5S_2$, $^5F_4 \rightarrow {}^5I_7$, or, in another way, 'borrowing' phonons from the host going to upper states. The first path ends up in the $^5I_7$ state. We know from our previous observations [15], based on the ESA spectra, that the

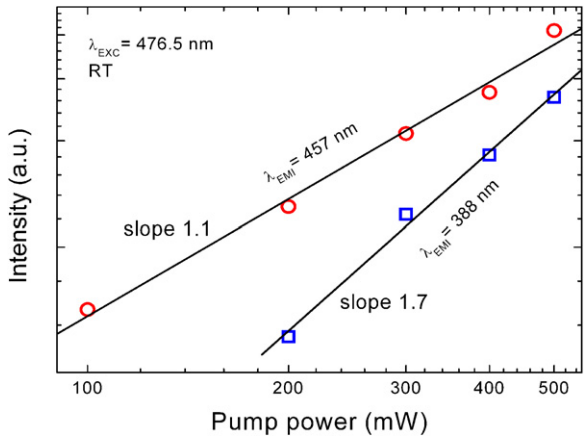

Figure 4. Slope characteristics for both anti-Stokes emissions.

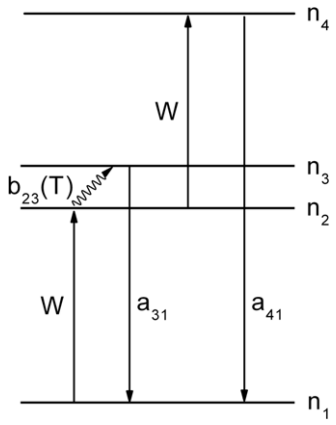

Figure 5. Simplified, four-level energy scheme used in kinetic analysis.

$^5I_7$ state gathers 76% of the population under CW excitation. The second path mentioned ends up in the $^5G_6$, $^5F_1$ states. Note that the above two paths compete with each other. Those ions which are transferred to the $^5G_6$, $^5F_1$ states are 'lost' for the $^5I_7$ state and vice versa. Then, the next act of the process occurs: emission from the $^5G_6$, $^5F_1$ states and excited state absorption (ESA) of the pumping line from the $^5I_7$ state. The latter transfers ions to the $^5G_4$, $^3K(2)_7$ states responsible for the 388 nm upconverted emission.

To make sure if such a model is justified, we performed additional measurements which could provide information about how many photons partake in the excitations leading to both observed anti-Stokes emissions [20, 21]: the dependence of the intensities of our anti-Stokes emissions on the excitation power. Figure 4 presents how the familiar formula $I_{\mathrm{EMI}} \propto P^m$ (where I_{EMI} is emission intensity, P is excitation power, and m is the number of photons involved in emission excitation) fits the obtained experimental data. The data are presented on a log–log scale. The resulting slopes show that the 457 nm emission is due to one photon absorption whereas 388 nm emission occurs after excitation engaging two photons. A possible undervalue (1.7 instead of 2.0) is probably not caused by saturation effects [21], but presumably by the sample temperature increase with the pumping power, which, as we know, diminishes the intensity of the 388 nm emission. The result shown in figure 4 agrees well with our model.

To ease further kinetic analysis we have simplified the scheme from figure 3 to the four-level scheme depicted in figure 5. In this model the level with population n_2 represents either the excited $^5F_3$ state or $^5S_2$, $^5F_4$, and $^5I_7$ states, since in CW conditions we deal with effective deexcitation (radiationless and then radiative) ending up in the $^5I_7$ state. The remaining '$n_{1,3,4}$' levels correspond to the $^5I_8$; $^5G_6$, $^5F_1$, and $^5G_4$, $^3K(2)_7$ states respectively. We have also omitted possible radiationless $|4\rangle \rightarrow |3\rangle$ transitions because their probability is estimated as lower or of the same order as others taking part in the process, but the population involved is much smaller than after the first step of excitation, hence only a very small part of the excited population goes back to the $|3\rangle$ state. Owing to these facts it also does not influence the measured slope characteristics.

In the frame of four levels, the kinetics of the system can be described by the following set of rate equations:

$$\begin{aligned} \dot{n}_1 &= -Wn_1 + a_{31}n_3 + a_{41}n_4 \\ \dot{n}_2 &= Wn_1 - b_{23}(T)n_2 - Wn_2 \\ \dot{n}_3 &= b_{23}(T)n_2 - a_{31}n_3 \\ \dot{n}_4 &= Wn_2 - a_{41}n_4 \qquad \text{and} \qquad \sum_{i=1}^{4} n_i = n, \end{aligned} \tag{1}$$

where n_i are the populations of the states taking part in the process, W is the excitation parameter (pumping rate), and a_{ij} are spontaneous transition rates from $|i\rangle$ to $|j\rangle$ states. The term: $b_{23}(T) = b_{23}^0(\mathrm{e}^{\hbar\omega/kT} - 1)^{-p}$ is responsible for the MASE effect, b_{23}^0 is the stimulated transition rate at $T = 0$ K whereas p is the number of phonons of energy $\hbar\omega$ involved in the process. Under CW excitation we can consider only stationary solutions of the set (1). From our point of view only two population densities are interesting: n_3 and n_4. In the CW conditions they are responsible for the 457 and 388 nm emissions respectively. It is also obvious that in such conditions the emission intensities are proportional to the mentioned populations. The stationary solutions are as follows:

$$n_3(T) = \frac{Wn}{\frac{a_{31}W}{b_{23}(T)a_{41}}(2a_{41} + W) + a_{31} + W} \tag{2}$$

for 457 nm emission, and:

$$n_4(T) = \frac{Wn}{2a_{41} + W + b_{23}(T)\left(\frac{a_{41}}{W} + \frac{a_{41}}{a_{31}}\right)} \tag{3}$$

for 388 nm emission.

Figure 6 shows the best fit of the solutions (2) and (3) to the experimental data taken from the inset of figure 2. The best fit has been obtained with the following parameters: $a_{31} = 3.33 \times 10^5$ s^{-1}, $a_{41} = 1.43 \times 10^6$ s^{-1}, $b_{23}^0 = 2 \times 10^4$ s^{-1}, $p = 2$, $\hbar\omega = 580$ cm^{-1}, $W = 4 \times 10^2$ s^{-1}, and $n = 1.45 \times 10^{20}$ cm^{-3}. The parameters a_{31}, a_{41}, and

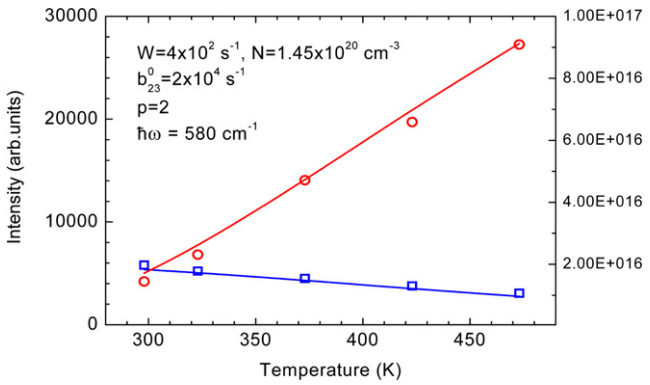

Figure 6. Fit of solutions (2) and (3) to the experimental dependence of the two anti-Stokes emissions on temperature.

$\hbar\omega$ are compatible with experimental data reported in [22] and [23–25] respectively. It is worth noting that when using one, three, or four phonons in the above analysis we could not obtain satisfactory fits. On the other hand, it seems that two phonons of the energy 580 cm^{-1} can span the energy gap between $^5F_3$ (actually, between the terminal level reached by 476.5 nm excitation) and $^5G_6$, $^5F_1$ states quite well, taking into account tail-ends of the state distributions. This gap is $\sim$1270 cm^{-1}, so that two phonons of 580 cm^{-1} (1160 cm^{-1}) can fit in with the gap.

4. Conclusion

The temperature dependent anti-Stokes emission intensities have been interpreted by means of the MASE effect, which causes the increase of one emission intensity being simultaneously the cause of the decrease of another, upconverted emission intensity. This competition has been analyzed by the kinetic approach and a satisfactory fit to the experimental data has been obtained. It is astonishing that such a simple model, as used, was capable of fitting the experimental data not only qualitatively, but also by means of the ratio of the 457 nm emission intensity increase slope to the slope of the decrease of the 388 nm emission intensity.

Acknowledgments

This work was supported by the Nicolaus Copernicus University (NCU) by the Grant of the NCU Rector, number 517-F. One of the authors (KW) was supported by the Polish Committee for Scientific Research (project PBZ/MEiN/01/2006/39). This work was also co-financed by the European Social Found and the state budget under the project 'Step into the future—scholarships for PhD students' of the Regional Council of Kujawsko-Pomorskie Province.

References

[1] Malinowski M, Piramidowicz R, Frukacz Z, Chadeyron G, Mahiou R and Joubert M-F 1999 *Opt. Mater.* **12** 409
[2] Cheng Zh X, Zhang Sh J, Han J R, Chen H Ch, Lu Q M and Guo H C 2001 *Cryst. Res. Technol.* **36** 449
[3] Ryba-Romanowski W 2003 *Cryst. Res. Technol.* **38** 225
[4] Yang X, Xiao S, Liu Z and Yan X H 2007 *Appl. Phys.* B **86** 77
[5] Rukmini E and Jayasankar C K 1995 *Opt. Mater.* **4** 529
[6] Kaczkan M and Malinowski M 2004 *J. Alloys Compounds* **380** 201
[7] Dereń P, Goldner P and Guillot-Noël O 2006 *J. Lumin.* **119/120** 38
[8] Liu Ch and Heo J 2006 *J. Non-Cryst. Solids* **352** 5325
[9] Malinowski M, Wnuk A, Frukacz Z, Chadeyron G, Mahiou R, Guy S and Joubert M-F 2001 *J. Alloys Compounds* **323/324** 731
[10] Wnuk A, Kaczkan M, Frukacz Z, Pracka I, Chadeyron G, Joubert M-F and Malinowski M 2002 *J. Alloys Compounds* **341** 353
[11] Wnuk A, Kaczkan M, Piramidowicz R, Mahiou R, Bertrand G, Joubert M-F and Malinowski M 2003 *Radiat. Eff. Defects Solids* **158** 469
[12] Kück S, Osiac E and Sokólska I 2005 *J. Opt. Soc. Am.* B **22** 323
[13] Osiac E 2002 *J. Alloys Compounds* **341** 263
[14] Auzel F 1976 *Phys. Rev.* B **13** 2809
[15] Piątkowski D, Wiśniewski K, Różański M, Koepke Cz, Kaczkan M, Klimczak M, Piramidowicz R and Malinowski M 2008 *J. Phys.: Condens. Matter* **20** 155201
[16] Koepke Cz, Wiśniewski K, Sikorski L, Piątkowski D, Kowalska K and Naftaly M 2006 *Opt. Mater.* **28** 129
[17] Mungan C E, Buchwald M I, Edwards B C, Epstein R I and Gosnell T R 1997 *Appl. Phys. Lett.* **71** 1458
[18] Edwards B C, Anderson J E, Epstein R I, Mills G L and Mord A J 1999 *J. Appl. Phys.* **86** 6489
[19] Hoyt C W, Hasselbeck M P, Sheik-Bahae M, Epstein R I, Greenfield S, Thiede J, Distel J and Valencia J 2003 *J. Opt. Soc. Am.* B **20** 1066
[20] Balda R, Mendioroz A, Fernandez J, Arriandiaga M A, Griscom L S and Adam J L 2001 *Opt. Mater.* **16** 249
[21] Pollnau M, Gamelin D R, Lüthi S R, Güdel H U and Hehlen M P 2000 *Phys. Rev.* B **61** 3337
[22] Kowalska M, Klocek G, Piramidowicz R and Malinowski M 2004 *J. Alloys Compounds* **380** 156
[23] Chen Y, Meichenin D and Auzel F 1995 *J. Phys.: Condens. Matter* **7** 3363
[24] Kenyon A J 2002 *Prog. Quantum Electron.* **26** 225
[25] Naftaly M, Batchelor C and Jha A 2000 *J. Lumin.* **91** 133